REPRESENTATION OF THE BODY IN THE LATERAL STRIATUM OF THE FREELY MOVING RAT: RESPONSIVENESS OF FAST SPIKING INTERNEURONS TO STIMULATION OF INDIVIDUAL BODY PARTS

By

JULIANNA KULIK

A thesis submitted to the

Graduate School-New Brunswick

Rutgers, the State University of New Jersey

In partial fulfillment of the requirements

For the degree of

Master of Science

Graduate Program in Psychology

Written under the direction of

Mark O. West

Approved by:

_____

_____

_____

New Brunswick, New Jersey

October, 2015

ABSTRACT OF THE THESIS

REPRESENTATION OF THE BODY IN THE LATERAL STRIATUM OF THE FREELY MOVING RAT:

RESPONSIVENESS OF FAST SPIKING INTERNEURONS TO STIMULATION OF INDIVIDUAL BODY PARTS

BY JULIANNA KULIK

Numerous studies have shown that certain types of striatal interneurons might play a crucial role in selection and regulation of striatal output. Among these, striatal Fast-Spiking Interneurons (FSIs) are parvalbumin positive, GABAergic interneurons that constitute less than 1% of the total striatal population. FSIs display a strong medial<lateral distribution gradient across the striatum, which suggests that they are important for regulation of motor functions subsumed within the lateral striatum. It is becoming increasingly evident that these sparsely distributed neurons exert a strong inhibitory effect on Medium Spiny projection Neurons (MSNs), the principal neurons of the striatum. MSNs in lateral striatum receive direct synaptic input from regions of cortex representing discrete body parts. Individual MSNs show phasic increases in activity during touch or movement of specific body parts. In the present study, we sought to determine whether lateral striatal FSIs identified by their distinct electrophysiological properties, i.e., short-duration spike and fast firing rate, display body part sensitivity similar to that exhibited by MSNs. Using a video recorded sensorimotor exam, each individual body part was stimulated and responses of single neurons were observed and quantified. Approximately half of the identified FSIs displayed patterns of activity related selectively to stimulation of discrete

body parts. Those patterns of activity were often similar to those exhibited by typical MSNs in the lateral striatum. Some FSIs displayed patterns of activity different from those described in for MSNs, such as a dramatic decrease in firing during movement of the related body part. Together these results serve as evidence that striatal FSIs process information related to discrete body parts and participate in control of motor output by the striatum.

Acknowledgements

This study was funded by NIDA grants 006886, 026252, 029873.

Special thanks to my committee for their guidance: Mark O. West, Tibor Koos, and Alexander Kusnecov

Special thanks to those who gave their time and energy assisting in this project: David Barker, Kevin Coffey, Joshua Stamos, Jackie Thomas, Alisa Ray, Anne Sokolowski, and the entire undergraduate research team.

Special thanks to my family for their support and patience:

Joanna Komorowska-Kulik, Bogdan Kulik and David Burkat

Table of Contents

List of Illustrations & Tables

Introduction

The striatum is the largest input structure of the basal ganglia, and is crucial for sensorimotor integration (Fairley & Marshall, 1986; Nakamura and Hikosaka, 2006; Samejima et al., 2005). Abnormalities in striatal functioning underlie a number of severe movement-related disorders such as Parkinson's disease, Huntington's disease, and Tourette's syndrome (Kalanithi et al, 2005; Ferrante et al., 1985; Richfield et al.,1995; Hallet et. al, 2000)

Medium Spiny Projection Neurons (MSNs) are the principal neurons of the striatum and constitute approximately 95% of its population (Groves, 1983; Rymar et al., 2004). MSNs receive synaptic input from virtually all areas of the cortex, thalamus and brain stem (Tepper & Plenz, 2006) and synapse in the globus pallidus and substantia nigra pars reticulata. MSNs also possess rich local axon collaterals (Kreitzer, 2009) and it has therefore been hypothesized that striatal output is controlled via lateral inhibition between MSNs (Groves , 1983; Kötter, Alexander & Wickens, 1995; Plenz ., Wickens, & Kitai, 1996). Nevertheless, inhibition between MSNs has been shown to be weak and therefore is unlikely to account for the magnitude of GABAergic inhibition that has been recorded from MSNs (Mallet, 2005; Jaeger et al., 1994; Tunstall et al., 2002; Koos et al., 2004; Mallet 2005; Plenz 2003).

Recent striatal research has targeted a class of GABAergic, parvalbumin positive interneurons, called Fast Spiking Interneurons (FSIs) (Kawaguchi et al., 1995) . FSIs are connected via gap junctions (Kita et al., 1990), and via numerous synaptic contacts onto MSNs within several hundred microns of their somata, can fire in synchrony and inhibit a large population of MSNs. Despite their presumed strong effect, FSIs constitute less than 1% of the striatal population. However, they are distributed more densely in the dorsolateral striatum (DLS) as compared to the medial striatum (Luk and Sadikot, 2001; Rymar et al., 2004). MSNs in the DLS receive direct synaptic input from regions of cortex representing individual body parts (Kincaid et al., 1998). As a consequence, clusters of neighboring Type IIb MSNs (Kimura, 1990) respond to stimulation or movement of the same body

parts (Liles & Updyke, 1985; Alexander & Delong, 1985; Carelli & West, 1991; Mittler et al., 1994; Cho & West, 1997). In acute preparations, parvalbumin positive neurons emit high frequency spikes in response to cortical stimulation, inhibiting neighboring MSNs (Bennett and Bolam, 1994; Gerfen, Baimbridge, & Miller, 1985; Kita et al. 1990; Parthasarathy & Graybiel 1997).

FSIs may be particularly important for controlling motor behavior via the inhibition of type IIB MSNs. Numerous questions arise regarding how the firing of FSIs might influence the relations of MSNs to body part stimulation, their clustering, their organization into a patchy somatotopy (Flaherty & Graybiel, 1993, 1994). However, no studies to date have examined FSI activity using the type of approach often used for studying MSNs, i.e., by testing responsiveness to stimulation of body parts in awake animals. To better understand whether FSIs exhibit any type of responsiveness, we recorded single neurons *in vivo* and tested the responding of FSIs during a sensorimotor body exam. As expected, the majority of recorded neurons exhibited electrophysiological characteristics typical of MSNs. A subset exhibited characteristics of FSIs that have been published by several laboratories (Berke et al. 2008, Gage et al., 2010, Wiltschko et al., 2010, Gittis et al., 2011), i.e., fast firing rates and narrow waveforms. This subset was preferentially recorded and tested. Given the reported sensitivity of FSIs to cortical input (Bennet & Bolam, 1994, Mallet et al., 2005, Parthasarathy & Graybiel,1997) and putative role in controlling surrounding MSNs, we anticipated that a proportion of FSIs in DLS would show changes in firing during stimulation or movement of individual body parts. Given the exclusive sign (increased firing) of change exhibited by MSNs in response to sensorimotor activity (Liles & Updyke, 1985; Alexander & Delong, 1985; Carelli & West, 1991; Mittler et al., 1994; Cho & West, 1997), we expected that some proportion of FSIs might show decreased firing centered on the onset of body part stimulation (i.e., that concomitant decreases in firing by FSIs might disinhibit MSNs), but given the reported sensitivity of FSIs to cortical input we also anticipated that some proportion of FSIs might show an increase in response to body part stimulation.

Methods

Subjects

Male Long Evans rats (N= 24*;* Charles Rivers Laboratories Wilmington, MA) took part in this study. Prior to surgery, animals were individually housed on a 12 hour light/dark cycle with lights on from 10:00 a.m. to 10:00 p.m. Animals were given *ad libitum* water and restricted food access to maintain body weight of 350g. All protocols were performed in compliance with the Guide for the Care and Use of Laboratory Animals (NIH, Publications 865–23) and were approved by the Institutional Animal Care and Use Committee, Rutgers University.

Procedures

Surgery

Animals were initially anesthetized with sodium pentobarbital (50 mg/kg, i.p.). Anesthesia was maintained by administering ketamine hydrochloride (60 mg/kg, i.p.) and sodium pentobarbital as needed. Atropine methyl nitrate (10 mg/kg, i.p.) and penicillin G (75,000 U/0.25 ml, i.m.) were administered to prevent respiratory arrest and post-surgical infection, respectively.

Twenty animals were implanted with a 16 microwire array (Micro-Probes, Gaithsburg Maryland) targeting the right dorsolateral striatum (2.0- 2.1 mm AP; 2.9- 3.5mm ML; mm -3.9 DV from Bregma). Each microwire array comprised sixteen (2x8) Teflon-insulated microwires (diameter: 50 μm, anteroposterior spacing: 0.35 mm, mediolateral spacing: 0.5 mm). An insulated ground wire was implanted 5 mm ventral from skull level in the contralateral hemisphere.

Four additional animals were implanted with Tungsten microelectrode arrays. Each microelectrode array consisted of a set of fifteen, 125 μm diameter microelectrodes and a ground wire. The microelectrode array was connected to an EDDS microdrive system, enabling post-surgical repositioning of the array along the DV axis. The maximum depth of lowering was 7 mm from the skull level. The ML and AP coordinates for implanting the microelectrode array were identical to those for implanting the microwire array. Each array was initially

lowered 1.5 mm below the skull level. The array casing was sealed to the surface of the skull with cyanoacrylate and attached to the front and back skull screws using dental cement.

Recovery took place in individual Plexiglas chambers, which served as the animals' home cages and recording cages for the duration of the experiment. Animals were provided food and water to maintain a healthy body weight of approximately 350g.

Body exam

After 8 days of post-surgical recovery, all animals underwent a body exam during which individual body parts (head, chin, neck, trunk, forelimb, forepaws, whiskers) were stimulated (gently poked or touched) using a cotton swab. Stimulation of each body part was performed repeatedly over the period of one hour. Each body part was stimulated at least ten times in a single series (further details are described in Carelli & West, 1991). Video recordings of body exams were time-stamped (30 frames/sec) by the same computer that time-stamped neuronal discharges.

To confirm spiking during each individual body part stimulation or body part movement, neuronal signals were recorded, amplified, and played through a pair of headphones. Body part sensitivity was judged during the body exam through auditory inspection of the neuronal activity heard through the head phones. (Carelli & West, 1991). For a neuron to be considered body part sensitive, a noticeable change in firing was required during the active or passive manipulation of that body part selectively. Using video recordings of the exam, recorded neural data were quantified post hoc with raster plots centered on the onset of each discrete body part stimulation.

Microwire Array Recordings

On the day of or the day after the body exam, data for spontaneous firing rates and waveform parameters were obtained by connecting animals to a recording harness at the onset of the light cycle and recording for a period of an hour while the animal was uninterrupted by body exam procedures.

Microdrive Recordings

Four animals implanted with movable microelectrode arrays underwent a slightly modified procedure. Eight days following surgery, each animal was connected to a recording harness and the microelectrode array was slowly lowered (~70 µm per minute) until neurons were first detected. The number and firing rate of cortical neurons was characterized at each point during the lowering of the array. The number of turns until the “quiet zone” (Carelli and West, 1991), corresponding to the corpus callosum, was estimated and the array was lowered further until spiking striatal neurons were detected. Each time the array was lowered by a quarter of a turn (70µm), the number of neurons observed was recorded and their profile was characterized. The array was lowered until it detected neurons matching the criteria of FSIs. i.e.,narrow waveform and fast firing. If a neuron matching the criteria of an FSI was observed, a body exam, identical to one for animals with microwire implants, was conducted. Neurons matching the criteria of FSIs were targeted for the body exam. After the body exam was complete, recording continued for a period of an hour to gather data consisting of spontaneous firing rates and waveform parameters uninterrupted by body exam. At the end of each day the array was lifted until cortical neurons were detected.

Fluorescent Immunohistochemical labelling

Following all recordings (30 days after surgery) animals were deeply anesthesized and perfused transcrandially with 0.9% phosphate buffered saline followed by 4% paraformaldehyde. Brains were post-fixed for 48 hours in 4% paraformaldehyde and subsequently transferred to a 30% sucrose solution. Brains of animals implanted with microwires were sliced into 30 µm coronal sections, whereas brains implanted with tungsten microelectrode arrays were sliced into 50 µm coronal sections. Fluorescent immunohistochemistry was performed on free floating brain tissue. Slices were incubated for an hour in a 4% Bovine Serum Albumin (BSA) and 0.3% Triton X-100 in phosphate buffer. 30 µm thick sections were rinsed and incubated overnight in a 4% BSA with mouse anti-parvalbumin antibody and rabbit anti-GFAP antibody. Next, tissue was rinsed and

incubated in anti-mouse secondary antibody conjugated to a green fluorophore (Alexa Fluor ® 488) and an anti-rabbit antibody conjugated to a red fluorophore (Alexa Fluor ®555). Subsequently, tissue was washed with phosphate buffer (PB) and mounted on a slide using mounting medium containing Dapi (nucleic acid stain), which served as a counter stain. Fifty µm thick slices were incubated only in anti-GFAP antibody and subsequently Alexa Fluor®555. All pictures were recorded with a Zeiss Axiovert 200M, Fluorescence microscope.

Tracing microwire tracks made use of the brain's natural immune reaction to the chronic presence of microwires – i.e., glial scarring. The process of glial scarring involves microglia that respond first near the place of the injury and astrocytes that increase their production of glial fibrilary acidic protein (GFAP) (Fawcett, 1999). The microglia and astrocytes are the main molecular component of a final glial scar (Fawcett, 1999). This astrocytic glial scar starts to form at the moment of an injury, when microwires are implanted, and is completed 10 days after surgery. In order to trace the tracks from the microelectrodes, an array was lowered to the maximum depth after the end of the recording and left for about ten days. The presence of astrocytes with upregulated GFAP along the entire length of microwires allowed us to trace microwire tracks by staining for GFAP protein (Polikov, 2006).

Analyses

Neural data

Following recording sessions data were displayed for assessment of waveform stability on a computer simulated oscilloscope. Parameters such as peak time, peak amplitude, spike time, spike height, and principle component analysis were used to detect and isolate neural spikes. Neuronal signals were considered recorded from one single neuron only if the following criteria were met: (1) Signals recorded from the same wire were of similar amplitude and shape. (2) The putative neuron exhibited a signal-to-noise ratio greater than 2:1. (3) The auto-correlation revealed a minimum interspike interval (ISI) ≥ 1.6 ms (natural refractory period). A cross-correlation was performed if several waveform

profiles were detected in the recordings from a single microwire. Waveforms were designated as belonging to two separate neurons if each individual waveform showed a refractory period containing zero spikes within 1.6 ms and discharges occurred within the first 1.6 ms in the cross-correlation. Otherwise, the signals were combined and considered originating from one single neuron.

Cluster Analysis

For each averaged neuronal waveform three parameters were computed: the neuron's average FR, the waveform's valley to peak length (μsec) and valley width (μsec). A cluster analysis, using SAS PROC CLUSTER, was conducted on these three standardized waveform parameters using average linkage based on Euclidian distances. A plot of pseudo *F* statistics was used to determine the cutoff for the number of clusters to retain. In order to be conservative in our analyses, neurons with firing rates slower than 2 spikes per second were not considered FSI-candidates (Wiltschko et al. 2010).

Body Exam Analyses

During body exams, each body part was designated as either a 'Unrelated' or 'Related' by the experimenter. Related body parts were designated as those that produced a detectable change in firing rate when stimulated, while Unrelated body parts were designated as those that did not produce any detectable change. A trial was defined as a single stimulation of an individual body part. The onset and offset of each individual stimulation was subsequently established using post-hoc video analysis. Firing rate from onset to offset of the stimulation period was designated as 'Test' firing while baseline firing was computed as firing rate during the 500 ms prior to the onset of stimulation. For each stimulus, change in firing rate from Baseline to Test period was assessed by computing a fold-change statistic in which the larger FR of the two, Baseline or Test, was divided by the other. A sign of change was applied to accommodate either increasing or decreasing Test FRs with respect to Baseline FR, such that if Baseline FR was greater than Test FR, then Baseline FR to Test FR ratio was given a negative sign of change. On the other hand, if Test FR was greater than Baseline FR, then Test FR to Baseline FR ratio was given a positive sign of

change. The change in the magnitude of FR was analyzed by taking the absolute value of the fold-change statistic (|fold-Δ FR|). The absolute values of the fold-changes in FR were collapsed across all trials within a test session by using the trimmed mean (10%). The trimmed mean data for firing rate changes were analyzed using a one-way mixed model ANOVA to analyze the trimmed means of the fold-changes in FR between the Unrelated and Related responses. Neuron was specified as a random effect, and Unrelated and Related stimulations associated with an individual neuron were nested together. Post-hoc one way t-tests using Sidak's Type I error correction were conducted by way of confidence intervals in which the means for Unrelated and Related were tested against a value of 1 (fold-change = 1 indicates no change from Baseline to Test). All analyses were conducted using SAS PROC GLIMMIX.

To investigate a possible dependency between MSN and FSI firing rates, the FR recorded during the 500ms pre-stimulus period of all FSIs with a 'Related' body part were first sorted into two categories depending on whether the MSN(s) recorded simultaneously was firing or not (0 FR or FR >0), and then averaged within-category.

Results

Six hundred forty-eight striatal neurons were recorded and 92 waveforms were isolated during offline spike sorting to undergo further analysis (the remainder exhibited characteristics of MSNs, characterized extensively via body exam in previous studies). Sixty of the isolated striatal neurons were sampled with microwire arrays and 32 neurons were sampled with microelectrode arrays. All 92 isolated neurons were entered into a cluster analysis to obtain an objective breakdown and subgrouping of the neural population. The cluster analysis revealed that the average neuronal waveforms could be grouped into eight discrete clusters based on the pseudo *F* statistics (see Figure 3 for cluster dendrogram). Post-hoc graphical analyses revealed that there were two main clusters that encompassed 62.6% and 28.5%, respectively, of the entire set of neurons (for a total of 91.2%). The 26 neurons grouped together into the smaller cluster had a distinctive, sharp waveform shape, with a short valley width [M=58.41μs (±3)], as well as short valley-to-peak latency [M=110 μs (±4)] and fast spontaneous firing rate [M=4.3 spikes per second (±0.9)], and thus were classified as FSIs. The 57 neurons in the larger cluster exhibited a waveform shape typical of MSNs with a broader valley width [M=81.05μs (±2.09)] and broader valley-to-peak latency [M=168.42, (±2.69)], as well as a slower spontaneous firing rate [M=1.11 spikes per second (±0.15)]. Figure 3 presents a scatterplot of data along those three dimensions. Figure 4 displays average overlaid waveforms separately for the two clusters of interest. Seventeen of the 26 neurons initially classified as FSIs showed firing rates higher than 2 spikes per second. Further analysis focused on those 17 neurons.

Of those 17 neurons, 9 received a thorough, video-recorded body exam. For 6 out of 9 neurons the body exam revealed a correlated body part to which the neuron selectively responded. The correlated body parts were the following: upward head movement (2 neurons), downward head movement, left whisker , snout, and left front paw. For 3 out of the 9 neurons the body exam did not reveal any body part with which the neuron was correlated (see Table 1 for types of unrelated and related body part with accompanying ranges of stimulation

applied).

The following analysis focused on the 6 neurons for which the body exam resulted in the experimenter's subjective determination that FR was selectively sensitive to stimulation of one body part ("related") but insensitive to other body parts ("control"). The |fold-Δ FR| values for the active and control body parts were entered into a mixed model ANOVA.

The mixed model ANOVA indicated a significant difference in the magnitude of FR change from Baseline to Test periods between Control and Related body parts, $F(1,11)=15.91$, $p=.0021$. Post-hoc Sidak t-tests indicated that Unrelated body part stimulation did not cause a significant change in magnitude of FR from Baseline to Test periods, $t(11)=0.78$, 99% CI [-4.31, 6.80]. In contrast, responses to stimulation of Related body parts showed a significant change in magnitude of FR from Baseline to Test periods, $t(11)=4.96$, 99% CI [2.97, 17.10]. These results provide statistical validation of the experimenter's qualitative assessments of FR change during the body exam, which have been consistently applied to studies of striatal MSNs, extended here to FSI for the first time. Results of analyses comparing FR's of FSIs depending on whether MSN was firing or not (FR=0 OR FR>0) showed a trend toward a negative (reciprocal) relationship, as the theory predicts, but it was not significant.

Discussion

Striatal FSIs are shown here to exhibit altered firing rates during movement or touch of discrete body parts. Previous studies have shown that in DLS there are somatotopically organized, 3- dimensional clusters of MSNs (~300$_{\mu m}$ across) sensitive to movement or touch of a specific body part (e.g., whiskers, front paw, back, head) (Liles & Updyke, 1985; Alexander & Delong, 1985). Approximately 50% of striatal MSNs display firing patterns that are altered by movement or touch of specific body parts.(Carelli & West, 1991; Mittler et al., 1994; Cho & West, 1997) Striatal FSIs show in vitro strong inhibitory effects on MSNs (Koos and Tepper, 1999) and FSIs are relatively enriched in DLS (Rymar et al., 2004). However no study thus far has attempted to investigate whether FSIs display altered firing patterns during a somatic sensorimotor body exam. The present large sample of neurons yielded a small subset that met criteria widely recognized as characteristic of striatal FSI (high firing rates, short valley durations, short valley to peak durations). The clear, selective responsiveness to body part stimulation by a proportion of those neurons provides the first evidence during behavior that discrete body parts are represented by the firing of striatal FSIs.

Neurons in the statistical cluster analysis designated as FSIs exhibited characteristics distinct from those of typical MSNs recorded in the DLS and therefore are unlikely to be MSNs. Because parvalbumin interneurons are the second most numerous class of neurons in the DLS, and the characteristics of neurons within that cluster were highly consistent, it is most reasonable to assume that those neurons were parvalbumin interneurons. Nine out of the 17 neurons classified as FSIs were carefully tested with a thorough somatic sensorimotor body exam. Six of the 9 recorded neurons responded selectively to stimulation of one individual body part. Three neurons exhibited clear and selective increases in firing rate during stimulation: upward head movement, downward head movement and whiskers, respectively. Those increases in activity were not dissimilar to responses of typical MSNs to movement or stimulation of the related body part (Figure 5): 1) the magnitude of change was

an increase on the order of several spikes per second from baseline; 2) increases were selective in nature with respect to the stimulated body part. For example the vibrissae sensitive FSI did not show altered firing during snout or peri-oral stimulation; 3) selectivity was also found for the direction of movement. Neurons showing an increase during downward head movement did not display any changes in firing during horizontal or upward head movement (Figure 6).

According to feed-forward inhibition theory as applied to the striatum, FSIs receive or respond to cortical input before MSNs do and delay or entirely abolish firing of MSNs (Koos and Tepper, 1999). Despite the fact that FSIs receive the same cortical input, the theory predicts that firing of pairs of FSIs and MSNs should be negatively correlated due to inhibitory effects of FSIs on MSNs. This has been observed in a number of studies where periods of high firing rate of an FSI were associated with decreased probability of an action potential in a neighbouring MSN (Gage et al., 2010). However in this study when FSI firing rates during baseline were separated according to MSN firing rate during the same time (MSN FR=0 or MSN FR>0), no difference in average FSI firing rate was observed (Figure 8). This assessment was capable only of revealing a general relationship between the two types of neurons in likelihood to fire. Testing more specific linkages was outside the present scope, given distances exceeding several hundred microns across the array of recording electrodes. Certain other results of the present study are in fact consistent with feed-forward inhibition theory. Notably, some proportion of FSIs, as indicated by the small sample observed in the present study, selectively and substantially decrease in activity during movement of an individual body part. This is in contrast with MSNs, which uniformly increase in activity during movement. FSIs showing decreases in firing could disinhibit MSNs, whereas FSIs that show increases in firing related to a movement could inhibit groups of MSNs representing body parts unrelated to that particular movement.

However, the relationship between FSIs and MSNs might not be as direct as predicted by the feed-forward inhibition theory of FSI-to-MSN synapses. There is evidence suggesting that other striatal interneurons might be involved in

modifying FSI-MSN synaptic connections (Koós and Tepper, 2002). Local inputs from cholinergic interneurons might be important for regulating activity of FSIs. Monosynaptic connections have been detected on FSIs from choline acetyl-transferase positive neurons in the rat striatum. In vitro studies have found that acetylcholine excites parvalbumin interneurons by acting on their nicotinic receptors (Koós and Tepper, 2002). At the same time acetylcholine has been found to decrease the inhibitory effect of FSIs on MSNs, by its action on presynaptic muscarinic terminals (Koós and Tepper, 2002). This suggests that acetylocholine neurons also play a major role in control of output selection from striatum.

In conclusion, we showed that FSIs exhibit robust changes in firing rate related selectively to stimulation of an individual body part. The majority of fully characterized FSIs showed changes in firing related to body part stimulation similar to those typically observed in MSNs. However, a subset of tested FSIs showed changes in firing rate that differed from those typically observed in MSNs. Two of the recorded neurons in this study showed decreases in activity related to movement of the related body part. The current study does not address the question of how sensorimotor responses of FSIs are related to those of MSNs. For this reason it is not yet possible to interpret the meaning of firing rate changes exhibited by FSIs during body part stimulation. Understanding of this relationship is a task for future in vivo and in vitro studies. Nonetheless, we have provided new information that now makes this question one that needs answering.

References

Alexander, G.E. & Delong, M.R. (1985). Microstimulation of the primate neostriatum. II. Somatotopic organization of striatal microexcitable zones and their relation to neuronal response properties. *Journal of Neurophysiology*, 53, 1417-1430.

Bennett, B. D., & Bolam, J. P. (1994). Synaptic input and output of parvalbumin-immunoreactive neurons in the neostriatum of the rat. *Neuroscience*, *62*(3), 707-719

Berke, J. D. (2008). Uncoordinated firing rate changes of striatal fast-spiking interneurons during behavioral task performance. *The Journal of Neuroscience*, *28*(40), 10075-10080.

Carelli, R. M., & West, M. O. (1991). Representation of the body by single neurons in the dorsolateral striatum of the awake, unrestrained rat. *Journal of Comparative Neurology*, *309*(2), 231-249.

Cho, J. & West, M.O. (1997). Distribution of single neurons related to body parts in the lateral striatum of the rat. *Brain Research*, 756, 241-246.

Fairley, P. C., & Marshall, J. F. (1986). Dopamine in the lateral caudate-putamen of the rat is essential for somatosensory orientation. *Behavioral neuroscience*, *100*(5), 652.

Fawcett, J. W., & Asher, R. A. (1999). The glial scar and central nervous system repair. Brain research bulletin, 49(6), 377-391.

Ferrante, R. J., Kowall, N. W., Beal, M. F., Richardson, E. P., Bird, E. D., & Martin, J. B. (1985). Selective sparing of a class of striatal neurons in Huntington's disease. *Science*, *230*(4725), 561-563.

Flaherty, A. W., & Graybiel, A. M. (1993). Two input systems for body representations in the primate striatal matrix: experimental evidence in the squirrel monkey. The *Journal of neuroscience*, 13(3), 1120-1137.

Flaherty, A. W., & Graybiel, A. M. (1994). Input-output organization of the sensorimotor striatum in the squirrel monkey. *The Journal of neuroscience*,*14*(2), 599-610.

Gage, G. J., Stoetzner, C. R., Wiltschko, A. B., & Berke, J. D. (2010). Selective activation of striatal fast-spiking interneurons during choice execution. *Neuron*,

67(3), 466-479.

Gerfen, C. R., Baimbridge, K. G., & Miller, J. J. (1985). The neostriatal mosaic: compartmental distribution of calcium-binding protein and parvalbumin in the basal ganglia of the rat and monkey. Proceedings of the National Academy of Sciences, 82(24), 8780-8784.

Gittis, A. H., Leventhal, D. K., Fensterheim, B. A., Pettibone, J. R., Berke, J. D., & Kreitzer, A. C. (2011). Selective inhibition of striatal fast-spiking interneurons causes dyskinesias. *The Journal of neuroscience*, *31*(44), 15727-15731.

Groves, P. M. (1983). A theory of the functional organization of the neostriatum and the neostriatal control of voluntary movement. *Brain Research Reviews*, 5(2), 109-132.

Hallett, J. J., Harling-Berg, C. J., Knopf, P. M., Stopa, E. G., & Kiessling, L. S. (2000). Anti-striatal antibodies in Tourette syndrome cause neuronal dysfunction. *Journal of neuroimmunology*, *111*(1), 195-202.

Jaeger, D., Kita, H.. & Wilson, C. J. (1994). Surround inhibition among projection neurons is weak or nonexistent in the rat neostriatum. Journal of Neurophysiology, 72(5), 2555-2558.

Kalanithi PS, Zheng W, DiFiglia M et al. (2005), Altered parvalbumin- positive neuron distribution in basal ganglia of individuals with Tourette syndrome. *Proc Natl Acad Sci* U S A 102:13307Y13312

Kawaguchi, Y., Wilson, C. J., Augood, S. J., & Emson, P. C. (1995). Striatal interneurones: chemical, physiological and morphological characterization. *Trends in neurosciences*, *18*(12), 527-535.

Kimura M (1990) Behaviorally contingent property of movement-related activity of the primate putamen. *J Neurophysiol* 63: 1277-1296.

Kincaid AE, Zheng T, Wilson CJ (1998) Connectivity and convergence of single corticostriatal axons. *J Neurosci* 18, 4722-4731.Kita, H., Kosaka, T., & Heizmann, C. W. (1990). Parvalbumin-immunoreactive neurons in the rat neostriatum: a light and electron microscopic study. *Brain research*, 536(1), 1-15.Koós, T., & Tepper, J. M. (1999). Inhibitory control of neostriatal projection neurons by GABAergic interneurons. *Nature neuroscience*, *2*(5), 467-472.

Koós, T., & Tepper, J. M. (2002). Dual cholinergic control of fast-spiking

interneurons in the neostriatum. *The Journal of neuroscience*, *22*(2), 529-535.

Koos, T., Tepper, J. M., & Wilson, C. J. (2004). Comparison of IPSCs evoked by spiny and fast-spiking neurons in the neostriatum. *The Journal of neuroscience*, 24(36), 7916-7922.

Kötter, R., Alexander, M. E., & Wickens, J. R. (1995). Effects of Asymmetric Neuronal Connectivity and Dopamine on Striatal Function: Simulation and Analysis of a Model for Huntington's Disease. In The Neurobiology of Computation (pp. 239-244). Springer US.

Kreitzer, A. C. (2009). Physiology and pharmacology of striatal neurons. *Annual review of neuroscience*, *32*, 127-147.

Liles, S.L. &Updyke, B.V. (1985). Projection of the digit and wrist area of precentralgyrus to the putamen: relation between topography and physiological properties of neurons in the putamen. *Brain Research*, 339(2), 245-255.

Luk, K. C., & Sadikot, A. F. (2001). GABA promotes survival but not proliferation of parvalbumin-immunoreactive interneurons in rodent neostriatum: an in vivo study with stereology. Neuroscience, 104(1), 93-103.

Mallet, N., Le Moine, C., Charpier, S., & Gonon, F. (2005). Feedforward inhibition of projection neurons by fast-spiking GABA interneurons in the rat striatum in vivo. *The Journal of neuroscience*, *25*(15), 3857-3869.

Mittler, T., Cho, J., Peoples, L.L. & West, M.O. (1994). Representation of the body in the lateral striatum of the freely moving rat: single neurons related to licking. *Experimental Brain Research,* 98, 163-167.

Nakamura, K., & Hikosaka, O. (2006). Role of dopamine in the primate caudate nucleus in reward modulation of saccades. *The Journal of neuroscience*, *26*(20), 5360-5369.

Parthasarathy, H. B., & Graybiel, A. M. (1997). Cortically driven immediate-early gene expression reflects modular influence of sensorimotor cortex on identified striatal neurons in the squirrel monkey. *The Journal of neuroscience*, *17*(7), 2477-2491.

Plenz, D. (2003). When inhibition goes incognito: feedback interaction between spiny projection neurons in striatal function. *Trends in neurosciences*, 26(8), 436-443.

Plenz, D., Wickens, J. R. & Kitai, S. T. (1996) in Computational Neuroscience, ed. Bower, J. M. (Academic, San Diego), pp. 397–402

Polikov, V. S., Block, M. L., Fellous, J. M., Hong, J. S., & Reichert, W. M. (2006). In vitro model of glial scarring around neuroelectrodes chronically implanted in the CNS. *Biomaterials*, *27*(31), 5368-5376.

Richfield, E. K., Maguire Zeiss, K. A., Vonkeman, H. E., & Voorn, P. (1995). Preferential loss of preproenkephalin versus preprotachykinin neurons from the striatum of Huntington's disease patients. *Annals of neurology*, *38*(6), 852-861.

Rymar, V. V., Sasseville, R., Luk, K. C., & Sadikot, A. F. (2004). Neurogenesis and stereological morphometry of calretinin- immunoreactive GABAergic interneurons of the neostriatum. *Journal of comparative neurology*, 469(3), 325-339.

Samejima, K., Ueda, Y., Doya, K., & Kimura, M. (2005). Representation of action-specific reward values in the striatum. Science, 310(5752), 1337-1340.

Tepper, J. M., & Plenz, D. (2006). Microcircuits in the striatum: striatal cell types and their interaction. In *Microcircuits: The Interface Between Neurons and Global Brain Function (Dahlem Workshop Reports)* (pp. 127-135).

Tepper, J. M., Tecuapetla, F., Koós, T., & Ibáñez-Sandoval, O. (2010). Heterogeneity and diversity of striatal GABAergic interneurons. *Frontiers in neuroanatomy*, *4*.

Tunstall, M. J., Oorschot, D. E., Kean, A., & Wickens, J. R. (2002). Inhibitory interactions between spiny projection neurons in the rat striatum. Journal of Neurophysiology, 88(3), 1263-1269.

Wiltschko, A. B., Pettibone, J. R., & Berke, J. D. (2010). Opposite effects of stimulant and antipsychotic drugs on striatal fast-spiking interneurons.*Neuropsychopharmacology*, *35*(6), 1261-1270.

Table 1 Presents the type of body parts tested, separated by responsive (Related) and non-responsive (Unrelated) as well as range for numbers of trials included in PETHs

Body Exam						
Neuron	Related	N Stimuli	Unrelated 1	N Stimuli	Unrelated 2	N Stimuli
1	Head Up	53	Left Forepaw	26	NA	NA
2	Head Up	26	Nose	33	Whisker	13
3	Left Paw	18	Head up	91	Back	10
4	Head Down	43	Head Sideways	43	Back	57
5	Whisker	97	Head Up	41	Left Paw	41
6	Snout	95	Head Up	52	Back	54

Figure Captions

Figure 1

a) Custom designed microelectrode array. b) Drivable microelectrode array with a custom designed microdrive.

Figure 2

a) a) & b) show overlaid single spike waveforms of an example MSN and d) displays its corresponding inter-spike interval histogram. c) represents overlaid mean waveforms of all recorded MSNs d) overlaid single spike waveforms of an example FSI with its corresponding ISI histogram (e) whereas f) shows overlaid mean waveform of 26 recorded FSIs. Red dashed line indicates measurements used for cluster analysis

Figure 3

Cluster analysis in the form of a dendrogram. The following variables were used for the cluster analysis: firing rate, valley and valley to peak durations. Cluster analysis with those variables yielded a solution with two main clusters comprising 95% of neurons.

Figure 4

Three-dimensional scatter plot showing an entire distribution of recorded waveforms along the three dimensions used in cluster analysis: firing rate, valley duration, valley to peak duration. Yellow dots represent 17 neurons classified as FSIs (with FR> 2 spikes per second), whereas dark red dots represent neurons classified as MSNs. Remaining neurons belong to minor clusters.

Figure 5

Peri-event time histograms (PETHs) displaying firing of body part responsive FSIs. a) PETH displays firing of a responsive neuron during downward head movement, whereas b) presents a response of the same neuron during upward head movement. The neuron is selectively responsive to downward head movement, exhibiting no response during upward head movement. c) another neuron classified as FSI during upward head movement. The neuron is clearly responsive to an upward head movement. d) shows activity of the same neuron during left paw movement.

Figure 6

FSIs that exhibited decreased firing rate related to movement or touch of a single body part. a) clear decrease in firing during passive movement of front left paw, whereas b) presents lack of modulation for the same neuron during passive head movement. c) clear decrease related to an upward head movement, whereas d) shows a lack of modulation for the same neurons during left paw upward

movement.

Figure 7

Mean absolute fold change in firing rate with respect to baseline, plotted separately for control body parts versus related body parts, showing clear difference between the two.

Figure 8

Grand average firing rate for FSIs, computed on the basis of a baseline period during body exam separately for trails when firing rate of MSN recorded simultaneously was equal to 0 vs trials when firing rate for MSN was greater than 0.

Figure 1

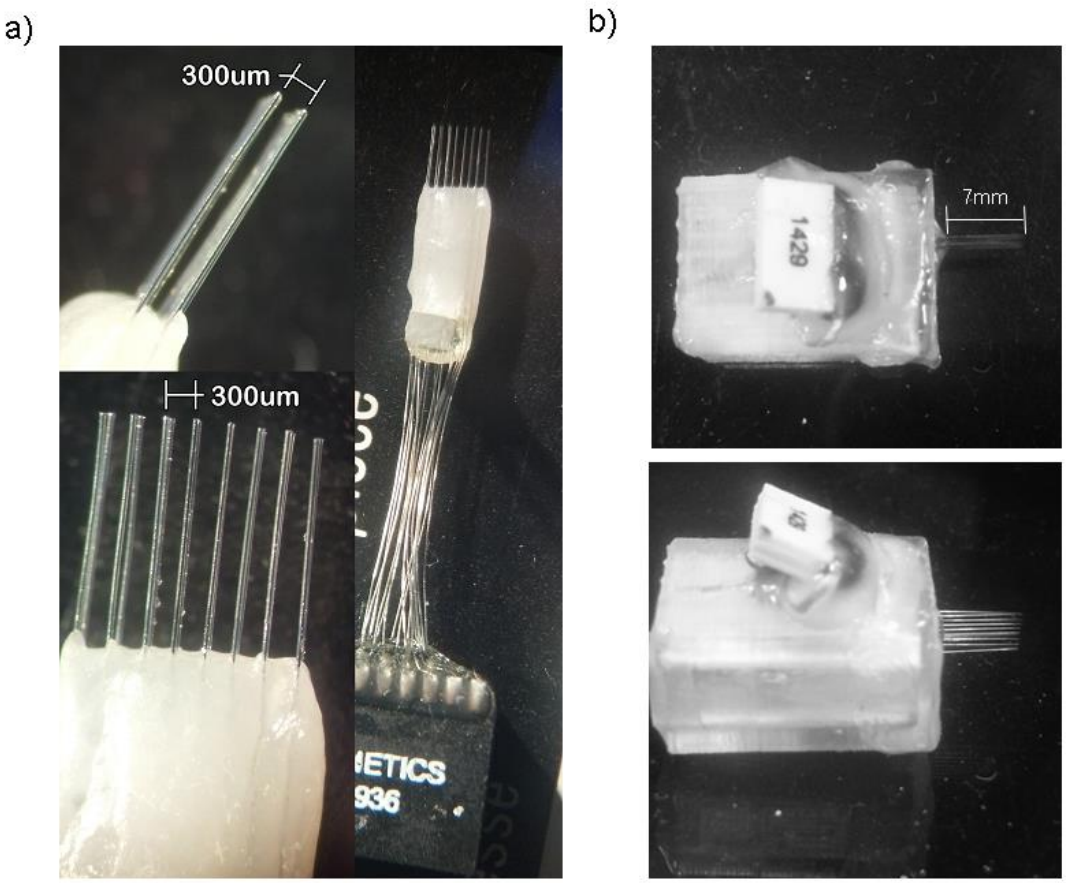

Figure 2

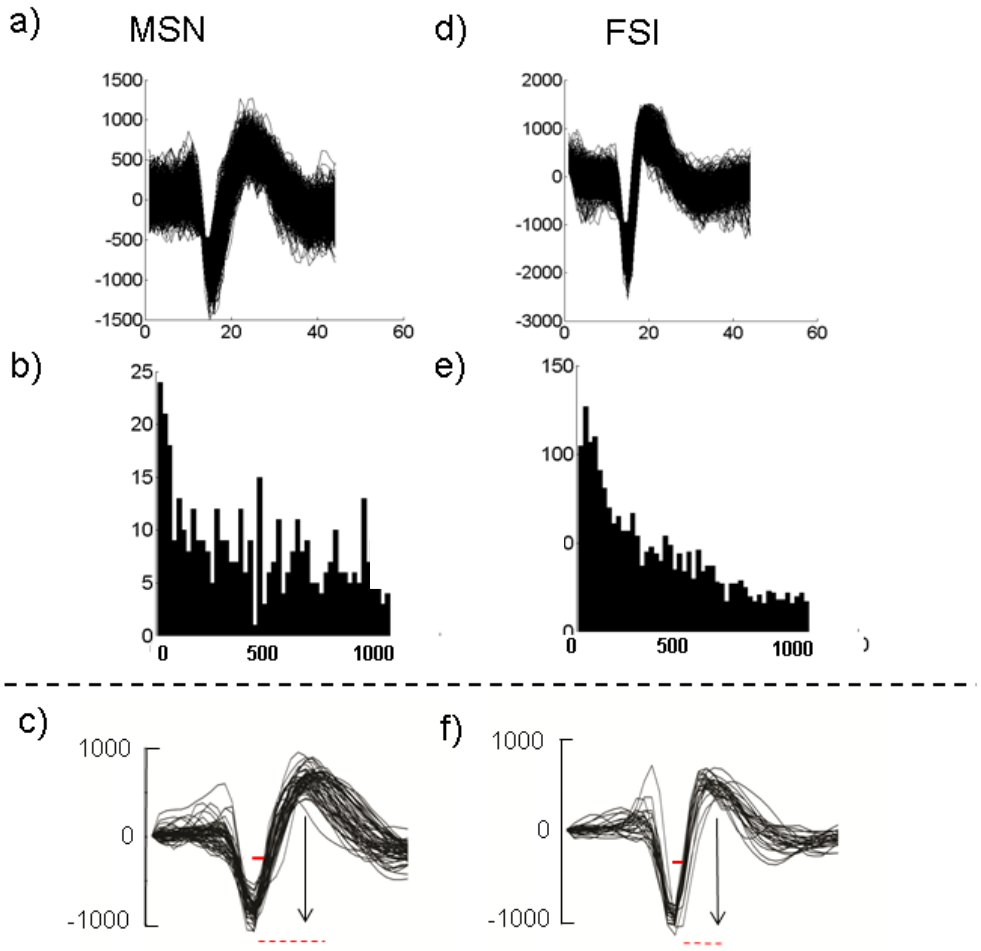

Figure 3

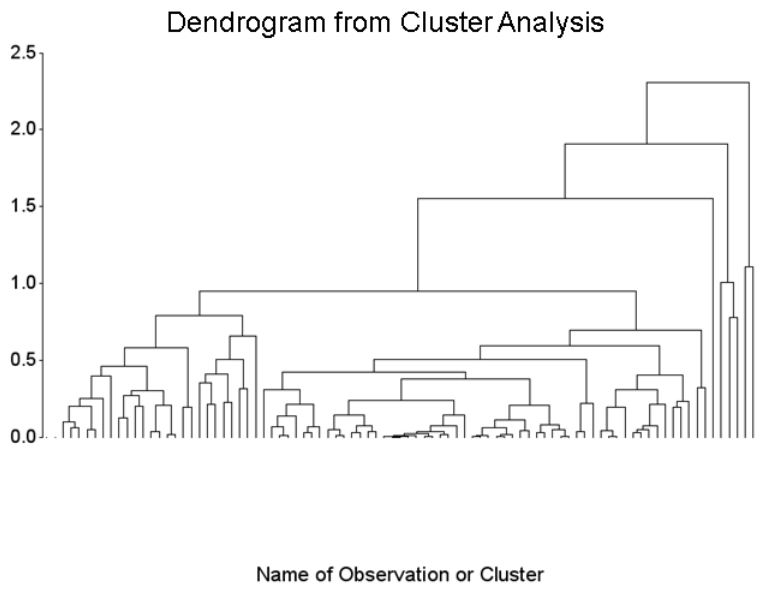
Dendrogram from Cluster Analysis
2.5
2.0
1.5
1.0
0.5
0.0
Name of Observation or Cluster

Figure 4

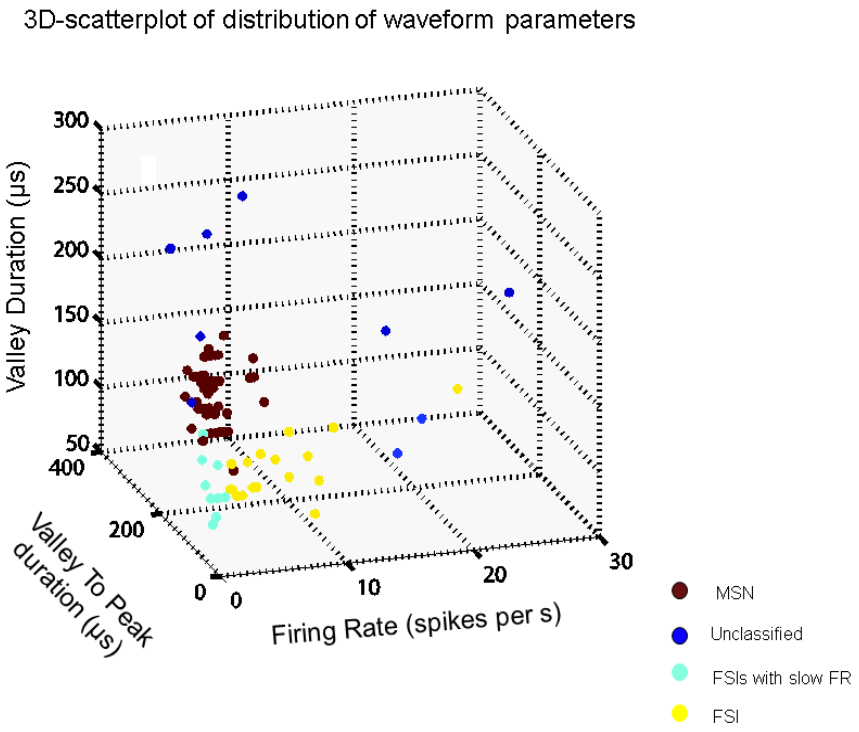
3D-scatterplot of distribution of waveform parameters
Valley Duration (µs)
300
250
200
150
100
50
Valley To Peak duration (µs)
400
200
0
0
10
20
30
Firing Rate (spikes per s)
MSN
Unclassified
FSIs with slow FR
FSI

Figure 5

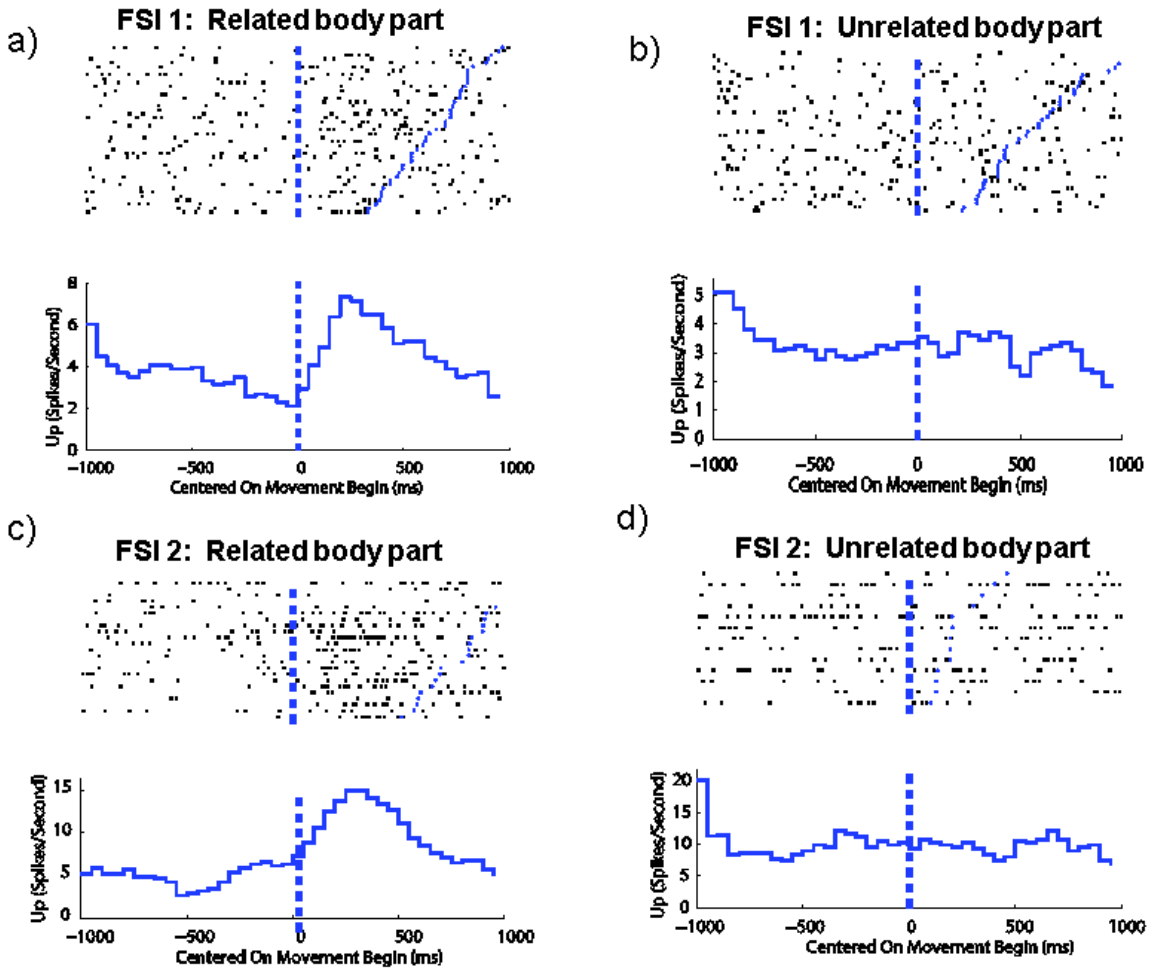
a)
FSI 1: Related body part
Up (Spikes/Second)
Centered On Movement Begin (ms)
b)
FSI 1: Unrelated body part
Up (Spikes/Second)
Centered On Movement Begin (ms)
c)
FSI 2: Related body part
Up (Spikes/Second)
Centered On Movement Begin (ms)
d)
FSI 2: Unrelated body part
Up (Spikes/Second)
Centered On Movement Begin (ms)

Figure 6

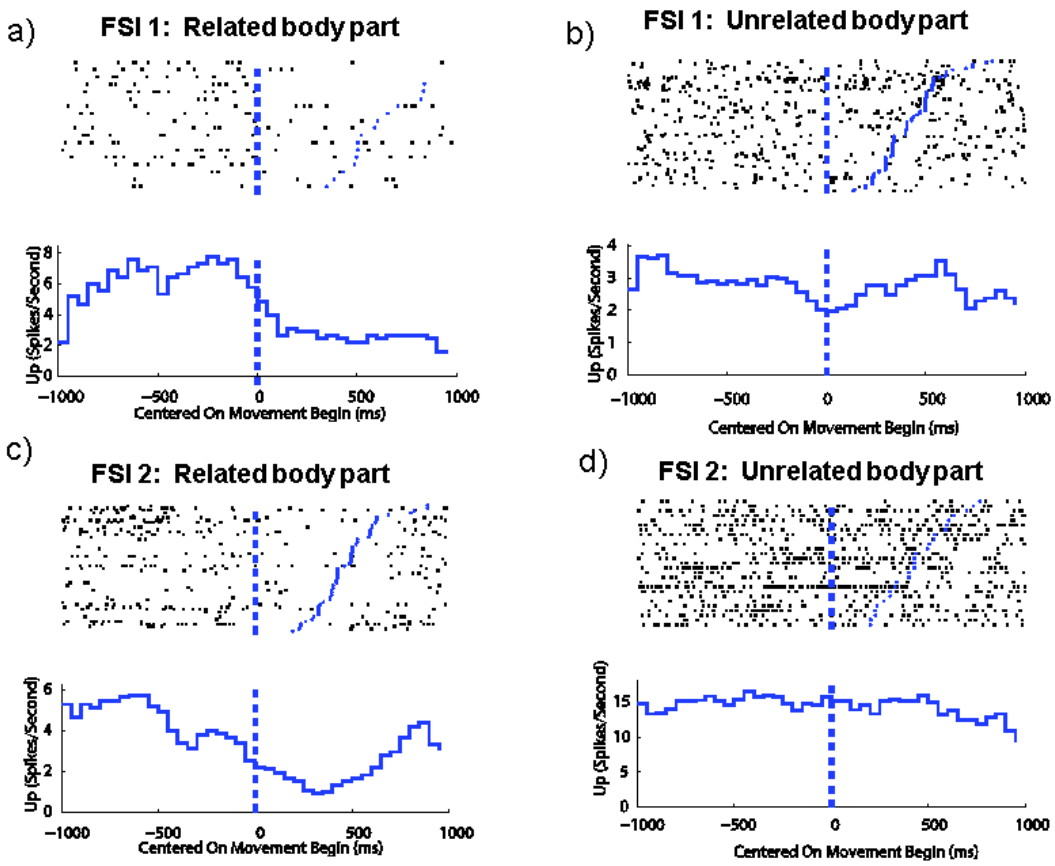
a)
FSI 1: Related body part
Up (Spikes/Second)
Centered On Movement Begin (ms)
b)
FSI 1: Unrelated body part
Up (Spikes/Second)
Centered On Movement Begin (ms)
c)
FSI 2: Related body part
Up (Spikes/Second)
Centered On Movement Begin (ms)
d)
FSI 2: Unrelated body part
Up (Spikes/Second)
Centered On Movement Begin (ms)

Figure 7

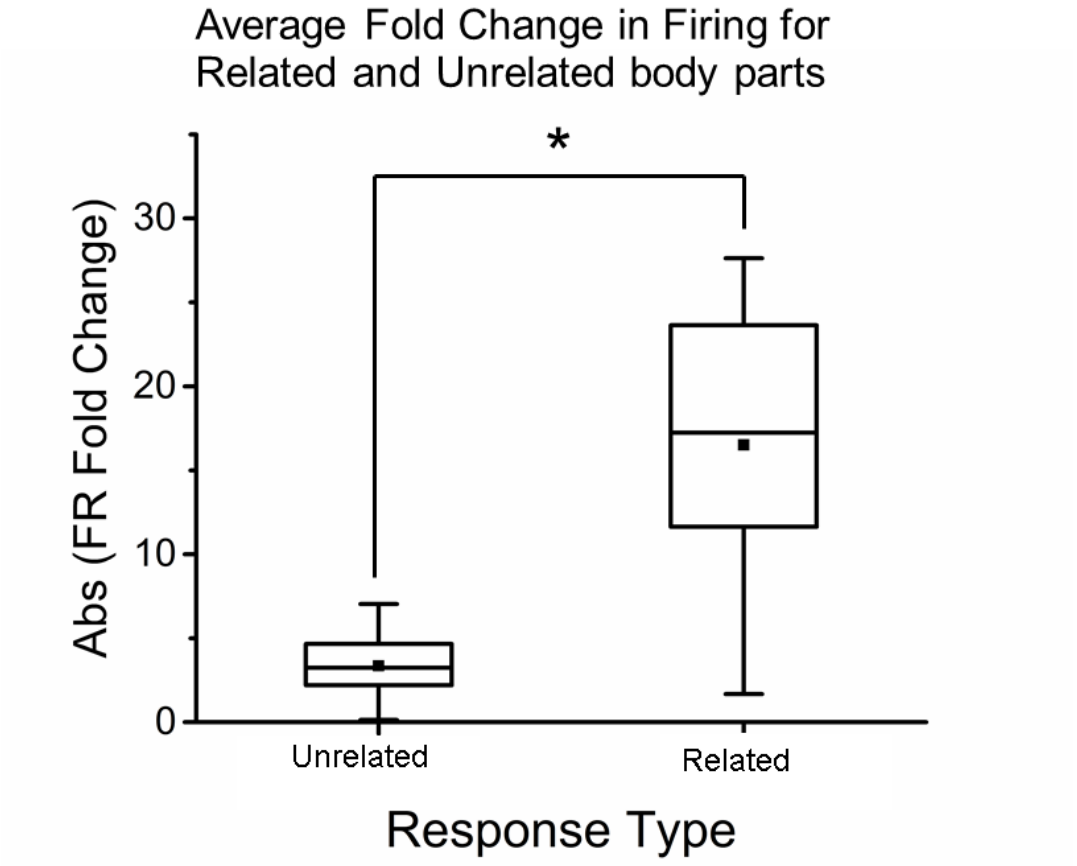
Average Fold Change in Firing for
Related and Unrelated body parts
*
Abs (FR Fold Change)
30
20
10
0
Unrelated
Related
Response Type

Figure 8